J. agric. Engng Res. (1996) **63,** 243–250

Soil Dynamics of Single and Multiple Tines at Speeds up to 20 km/h

P. N. Wheeler; R. J. Godwin

Silsoe College, Cranfield University, Silsoe, Bedford MK45, 4DT

(Received 10 April 1995; accepted in revised form 14 November 1995)

A force prediction model has been developed for single and multiple tines at speeds at which inertial effects are signficant. The soil worked by the tines is assumed to obey the Mohr–Coulomb criterion. The model can be extended to estimate the dynamic forces in adhesive soils by revising tine rake angle to account for geometry changes resulting from the soil body adhering to the tine.

Results of experiments carried out between speeds of 1 and 20 km/h are reported for both frictional (laboratory) and cohesive (field) soils and comparisons are made between theoretical and measured values. The predicted forces agreed with experimental data and in the majority of cases the magnitude of the difference between the predicted and experimental data was less than the least significant difference between treatment means at the 0·05 probability level.

Notation

c	cohesion, kN/m^2
c_a	soil-interface adhesion, kN/m^2
d	depth of tine from soil surface, m
d_i	depth of imaginary tine from soil surface, m
f	forward distance of soil beakout from tine at surface, m
q	surcharge pressure, kN/m^2 (assumed zero in this application)
m	rupture distance ratio
n	number of tines
r	crescent radius, m
s	lateral distance between the inside edges of adjacent tines, m
t	parameter used in testing differences in mean values[11]
v	velocity, m/s or km/h
w	width of tine, m
D	total horizontal force, kN
F	inertia component of the cutting force, kN
P	resultant passive force
H_t	horizontal force component, kN
H_{ti}	horizontal force component of the crescent failure of an imaginary tine, kN
V_t	vertical force component, kN (positive force downwards)
α	rake angle from the forward horizontal, deg
α_e	effective rake angle, deg
δ	angle of soil-interface friction, deg
ϕ	soil friction angle, deg
γ	soil bulk density, kN/m^3
β	soil shear plane angle, deg
N	dimensionless number

Suffixes to N

γ	gravitational
ca	cohesive and adhesive
a	inertial
q	surcharge

Presented at the Second International Conference on Soil Dynamics, Silsoe, Bedford, UK, 23–27 August 1994

1. Introduction

The speed at which soil engaging operations are conducted can have a significant effect on implement forces and therefore on the energy consumption above certain critical speeds. The inertia component of the cutting force (F) for an implement of width (w) and depth (d) can be determined by dimensional analysis where F/w is expressed as a function of v^2/gd. As the forward speed (v) in practice is often small this component has been ignored in many applications.[1] These assumptions were confirmed in studies with shallow blades by Schuring and Emori[2] who found that the effect of soil inertia is negligible at speeds of less than $\sqrt{5gw}$. Therefore, if this relationship was

0021-8634/96/030243 + 07 $18.00/0

assumed valid for a narrow tine of width 30 mm, the inertia forces would begin to have significance at speeds in excess of 4·36 km/h.

Godwin and Spoor[3] proposed a model for predicting both the horizontal and vertical soil forces acting on a tine and found agreement to within 15–20% of experimental values. The model was based upon the passive soil failure model of Hettiaratchi *et al.*[1] which assumed that at low speeds the inertia effects associated with accelerating soil from the front of the tine are insignificant. Subsequent work by Godwin *et al.*[4] extended this concept to predict the horizontal force on multiple interacting tines. McKyes[5] developed an equation to predict the forces acting on a wide blade that incorporated dynamic effects. The validity of the analysis was verified with respect to results from the work of Luth and Wismer[6] obtained using a blade of semi-infinite width moving at speeds between 1 and 10·8 km/h in an air-dried sand and showed a good correlation between experimental and theoretical values. The work of Stafford[7] produced a valuable insight into the behavior of tines at speeds up to 18 km/h, however a specific model for force prediction at higher speeds was not developed.

This paper outlines a method of adapting the dynamic force predictions of McKyes[5] to apply to narrow tines working above critical depth by modifying the model of Godwin *et al.*[4] to incorporate an inertial component. A simple modification to the model is proposed to broaden the range of soils for which force predictions can be made to include adhesive/cohesive conditions where soil scouring is not taking place.

2. Theory

2.1. *Dynamic force calculation*

The model of Godwin *et al.*[4] was used as a basis to predict the forces on single tines. The tine geometry indicated that the failure would be upward, forwards and sideways (above critical depth). Ignoring soil–metal adhesion effects, which are generally a very small proportion of the total force, the relevant part of the model gives the horizontal component (H_t) of the passive force (P) as

$$H_t = (\gamma d^2 N_\gamma + cdN_{ca} + qdN_q) \times [w + d(m - \tfrac{1}{3}(m-1))] \sin(a + \delta) \qquad (1)$$

The three terms in the first bracket account for gravitational, cohesive and adhesive, and surface surcharge loading effects respectively. The second bracket contains the tine width (w) and an additional

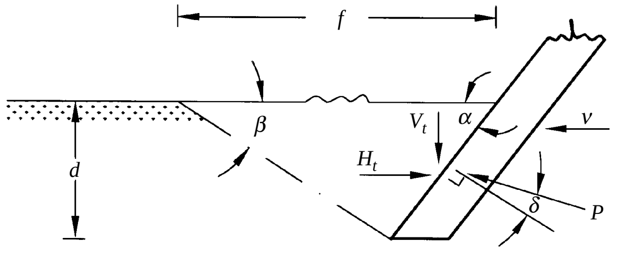

Fig. 1. Wide tine showing soil failure plane

term linked to depth (d) which allows for crescent failures at each side of the tine. The rupture distance ratio (m) relates the forward distance between the tine face and the rupture zone (f) to the depth of the tine (d) as shown in *Fig. 1*. The final term ($\sin(\alpha + \delta)$) gives the horizontal component of the resultant force.

A simplified equation for the vertical force component, V_t, is given by

$$V_t = (\gamma d^2 N_\gamma + cdN_{ca} + qdN_q) \times [w + d(m - \tfrac{1}{3}(m-1))] \cos(\alpha + \delta) \qquad (2)$$

The expression in the second bracket is less complicated than that originally given in the model by Godwin and Spoor[3] and produces a negligible difference in the vertical force component at rake angles less than 75% (when $\delta = 20°$) as shown in *Fig. 2*, the main difference occurring with the magnitude of the upward (negative) force at a rakge angle of 90°.

The above model has no allowance for speed effects. However, McKyes[5] developed an equation for the force P acting on a wide tine blade, given by Hettiaratchi *et al.*,[1] to include an inertial term as outlined by Luth and Wismer.[6]

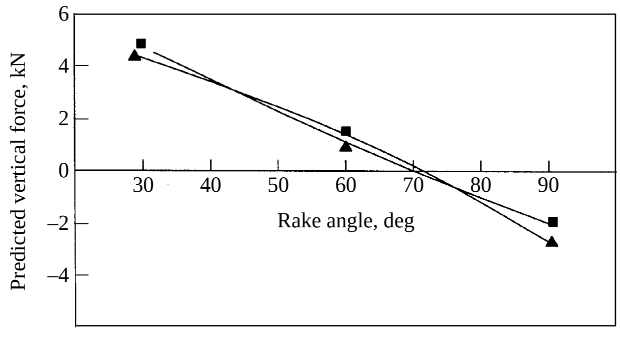

Fig. 2. Comparison of vertical force predictions from original (■) and simplified (▲) equations for a 0·03 m wide tine at 0·25 m depth in soil with $\phi = 30°$, $c = 30\ kN/m^2$ and $\delta = 20°$

If soil–metal adhesion (c_a) effects are ignored this equation is as follows

$$P = (\gamma d^2 N_\gamma + cdN_{ca} + qdN_q + \gamma v^2 dN_a)w \tag{3}$$

where

$$N_a = \frac{\tan\beta + \cot(\beta + \phi)}{(\cos(\alpha + \delta) + \sin(\alpha + \delta)\cot(\beta + \phi)) \times (1 + \tan\beta \cot\alpha)} \tag{4}$$

The angle β is not included in the model given by Godwin *et al.*[4] as the geometry of the soil failure is defined in terms of rupture distance ratio, (m). McKyes[5] assumed that the soil failure plane between tine tip and soil surface follows a straight line as shown in *Fig. 1*, from which β can be defined as

$$\beta = \arctan\left(\frac{1}{m - \cot\alpha}\right) \tag{5}$$

Data giving m values for different tine rake angles is available from Godwin and Spoor[3] and is summarized in *Fig. 3.*

It can be seen from Eqn (3) that the force associated with velocity change for wide tines is

$$F = \gamma v^2 dN_a w \tag{6}$$

This term is applicable to wide tines and is based upon inertial forces associated with accelerating a wedge of soil of width and depth equal to tine width and depth respectively. In order to apply this term to narrow tine theory, i.e. to incorporate the crescent edge effects, it was assumed that the inertia forces are generated in proportion to the volume and, hence, weight of the soil displaced by the tine, which reduces with depth, as shown in *Fig. 4*. This volume is estimated by considering the cross-sectional area of the disturbed soil immediately ahead of the tine which is given by (dw) as in Eqn (6) and for the two shaded crescent sections by $2(0{\cdot}6d^2/2)$, since the shaded region is typically 0·6 of the area represented by the triangle ABC. Therefore combining these concepts with Eqn (1) gives a total horizontal force component of

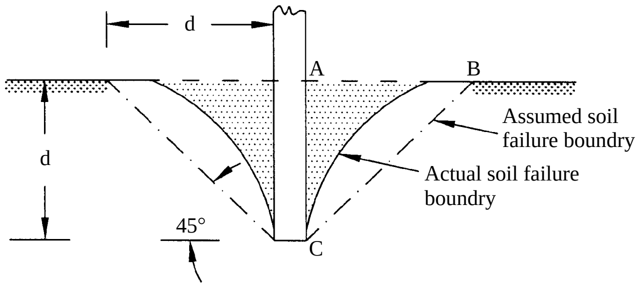

Fig. 4. Cross-section of typical tine failure soil profile

$$H_t = (\gamma d^2 N_\gamma + cdN_{ca} + qdN_q)[w + d(m - \tfrac{1}{3}(m - 1)) + \gamma v^2 N_a d(w + 0{\cdot}6d)]\sin(a + \delta) \tag{7}$$

Similarly the vertical force component (V_t) is given by

$$V_t = (\gamma d^2 N_\gamma + cdN_{ca} + qdN_{ca} + qdN_q)[w + d(m - \tfrac{1}{3}(m - 1)) + \gamma v^2 N_a d(w + 0{\cdot}6d)]\cos(\alpha + \delta) \tag{8}$$

2.2. *Effects of non-scouring conditions*

Eqn (7) gives the total horizontal force on a tine moving through soil, taking into account the effect of speed. It is based on the assumption that soil is scouring, i.e. sliding cleanly over the tine face. Obviously if scouring does not occur and soil builds up on the tine, the effective tool geometry will be altered and the equation can no longer be applied in this form.

Experience of tines running in cohesive clays shows that soil build up occurs near the surface but decreases with depth to the tine point as shown in *Fig. 5*. This means that the effective rake angle α_e is greater than

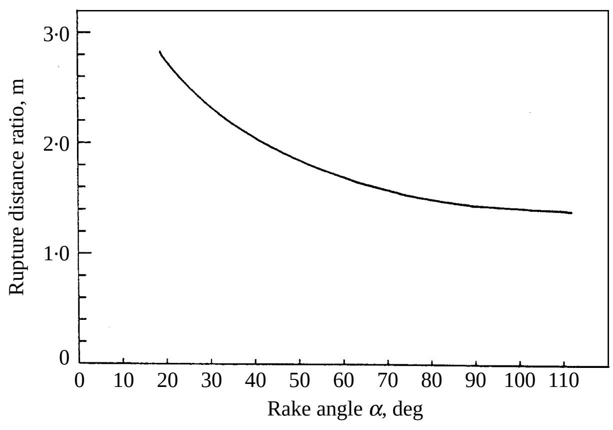

Fig. 3. Experimental relationship between rupture distance ratio (m = f/d) and tine rake angle (α) (after Godwin and Spoor[3])

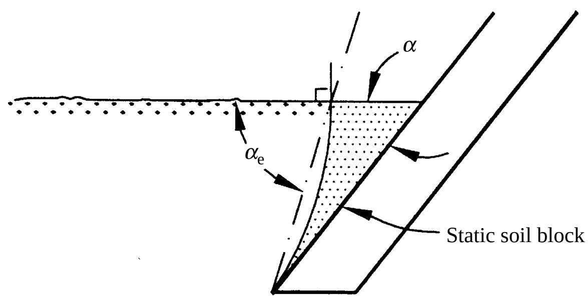

Fig. 5. Non-scouring (static) soil block on tine face

the actual tine angle α. A simple assumption was used in order to take this effect into account where α_e is the mean rake angle between α at depth and 90° at the soil surface, as given in Eqn (9)

$$\alpha_e = \frac{\alpha + 90}{2} \tag{9}$$

Hence, for non-scouring soils α_e replaces α and now because the moving soil slides over static soil the interface friction angle (δ) is assumed to be equal to ϕ.

2.3. *Multiple tines*

Sections 2.1 and 2.2 outlined the analysis of forces for a single working in soil, taking into account tine geometry, surface loadings, soil shear strengths, scouring and non-scouring and speed effects. The analysis provides a model from which the magnitude and direction of the resultant force can be calculated.

To allow force predictions for multiple tines, the single tine model was adapted by Godwin *et al.*[4] to include tine interaction effects. This involved a model where the draught forces of the individual tines were added together, with compensation made for the area of overlap shown shaded in *Fig. 6*. This is achieved by assuming the principle of superposition applies, which is the basis of many soil dynamic theories,[1,5] and subtracting an equivalent draught force required to disturb the interacting zone above and between the individual tine soil failure boundaries, referred to as the imaginary tine.

Assuming that the soil failure planes act at 45° to the horizontal, the imaginery tines, *Fig. 6*, have a depth of

$$d_i = d - \frac{s}{2} \tag{10}$$

and are assumed to have negligible width. The total horizontal force (D) for a group of (n) tines can, therefore, be calculated from

$$D = nH_t - (n-1)H_{ti} \tag{11}$$

Where H_{ti} is the horizontal force component of an imaginary tine.

This model accounts for tine spacing effects in the following manner, i.e. closer tine spacings produce greater imaginary tine depths and hence smaller values of total draught. The model assumes that providing soil can flow between the tines, then tine stagger (relative fore and aft positions) will not affect the soil forces.

3. Comparison between experimental and predicted forces

A series of experiments were conducted in both frictional soils (in laboratory conditions) and cohesive soils (in field conditions). In both conditions soil moisture content and bulk unit weight were determined gravimetrically; cohesion and internal friction were determined from triaxial tests and adhesion and soil metal friction by weighted sliding plane tests of Crowther and Haines.[8] The results of the soil analysis are summarized in Table 1.

Forces were measured using an octagonal ring transducer (Godwin[10]) linked to a signal conditioning and data logging unit via strain gauge amplifiers, each force was monitored at 100 Hz. When working in the laboratory the recorded sample time varied from 2 to 6 s depending on the forward speed of the study. When working in the field longer sample times of 6 to 10 s were used, again depending on test speed. The longer sample time was necessary due to more variable soil conditions in the field than in the laboratory.

The results of the single tine tests at 250 mm deep in

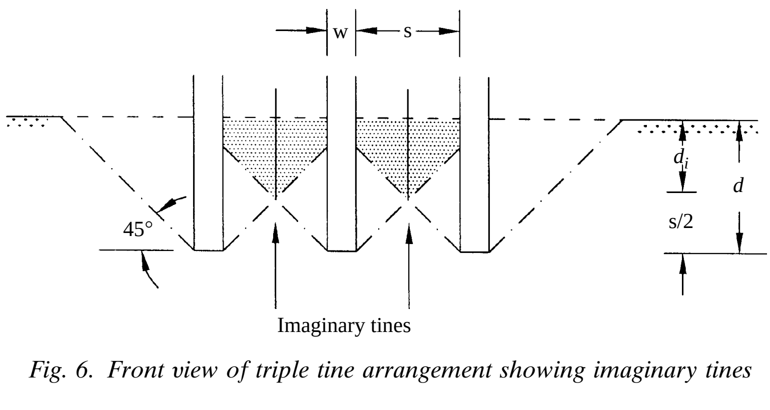

Fig. 6. Front view of triple tine arrangement showing imaginary tines

Table 1
Summary of soil properties

Soil property	*Units*	*Cottenham soil series* (Frictional soil)*	*Evesham soil series* (Cohesive soil)*
Moisture content (dry base)	%	8·7	36
Bulk unit weight, γ (dry base)	kN/m^3	14·9	16·7
Internal friction angle, ϕ	deg	30	8·6
Cohesion, c	kN/m^2	10	16
Soil metal friction, δ	deg	15	8·6
Sand	%	73	17
Silt	%	10	28
Clay	%	17	55

* See King.[9]

frictional and cohesive soils are shown in *Figs 7* and *8* respectively. All measured data points are the mean of at least four replications. In the frictional soil there is general agreement between predicted and measured values over the complete speed range. The magnitude of the differences in the horizontal force component is approximately equal to the magnitude of the least significant difference (l.s.d.) between treatment means, calculated from the experimental data at a probability level of 0·05 and shown as a vertical band. The least significant difference indicates the difference required in the mean force for each speed and rake angle for either to have a significant effect. It is calculated by multiplying the tabulated value of t (Ref. 11) (for the probability level and error degrees of freedom) and the standard error of the difference between treatment means resulting from an analysis of variance. There is greater variation between the experimental and predicted vertical force component, this is frequently two to three times the value of the least significant difference. In the cohesive soil under non-scouring conditions, predicted values show close agreement with the experimental results and in the majority of cases lie within a band width equal to the least significant difference or less. The exception to this difference is the predicted horizontal component of force for tines with rake angles of 40° in 5 km/h which is significantly underpredicted. There is a tendency for measured forces (particularly in cohesive conditions) to rise more rapidly than predicted forces in response to a speed increase i.e. predictions are correct at low speeds (1 km/h) and high speeds (20 km/h) but low in the mid range. This trend is also seen in the data on tine force variation in response to speed in cohesive soils in the work of Stafford[7] and may be a result of a change in the type of soil failure in front of the tine or changes in soil characteristics due to speed of shearing.

Also shown in *Figs 7* and *8* is the velocity of 4·36 km/h (indicated by the vertical short dashed line) as predicted by Schuring and Emori[2] below which it can be seen that the inertial component has little effect on the tine forces. Table 2 shows the speeds at which (1) a 5% and (2) a 10% rise in predicted horizontal and vertical force occurs. The mean speed vaues for 5% and 10% increases in horizontal and vertical forces for the tine rake angles studied in cohesive and frictional soil are 6·0 km/h and 8·4 km/h respectively. In all cases, the mean values for different tine rake angles are greater than the value of 4·36 km/h from the term provided by Schuring and Emori.[2] This is as expected as the original work did not take into account the effect of implement depth and the soil failure effects at each side of the tine.

As this study was conducted using tines of constant depth, the effect of depth on inertial forces cannot be determined. However, the effect of the soil failure effects at each side of the tine can be included by assuming the effective width of the soil body is $(w + 0{\cdot}6d)$ from Eqns (7) and (8) and hence the equation of Schuring and Emori[2] can be modified to $\sqrt{5g(w + 0{\cdot}6d)}$ for narrow tines. This gives an estimated critical speed of 10·7 km/h for 30 mm wide, 250 mm deep tines which is also shown in *Figs 7* and *8* (indicated by the vertical, long dashed line). This speed is equivalent to an average increase in predicted horizontal force of 19% and 14% for the frictional and cohesive soils respectively for the range of rake angles studied.

Fig. 9 shows the effect of tine spacing and speeds of 5 km/h and 20 km/h on horizontal forces acting on multiple tines with a rake angle of 40° in frictional

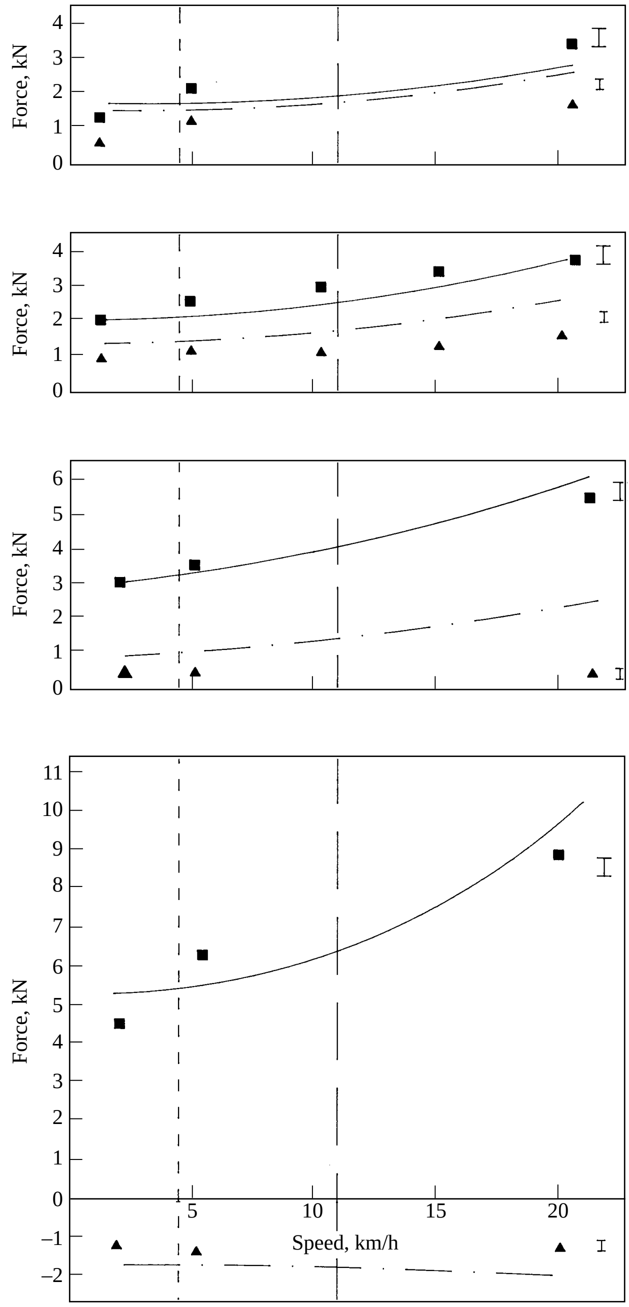

Fig. 7. Effect of speed on forces acting on a single tine with rake angle of 30° (top), 40° (upper centre), 60° (lower centre), and 90° (bottom) in frictional soil. Also shown are the l.s.d. bands at 0·05 probability level for the experimental data. ■, *Measured horizontal force component;* ▲, *measured vertical force component; ——, predicted horizontal force component; – · –, predicted vertical force component*

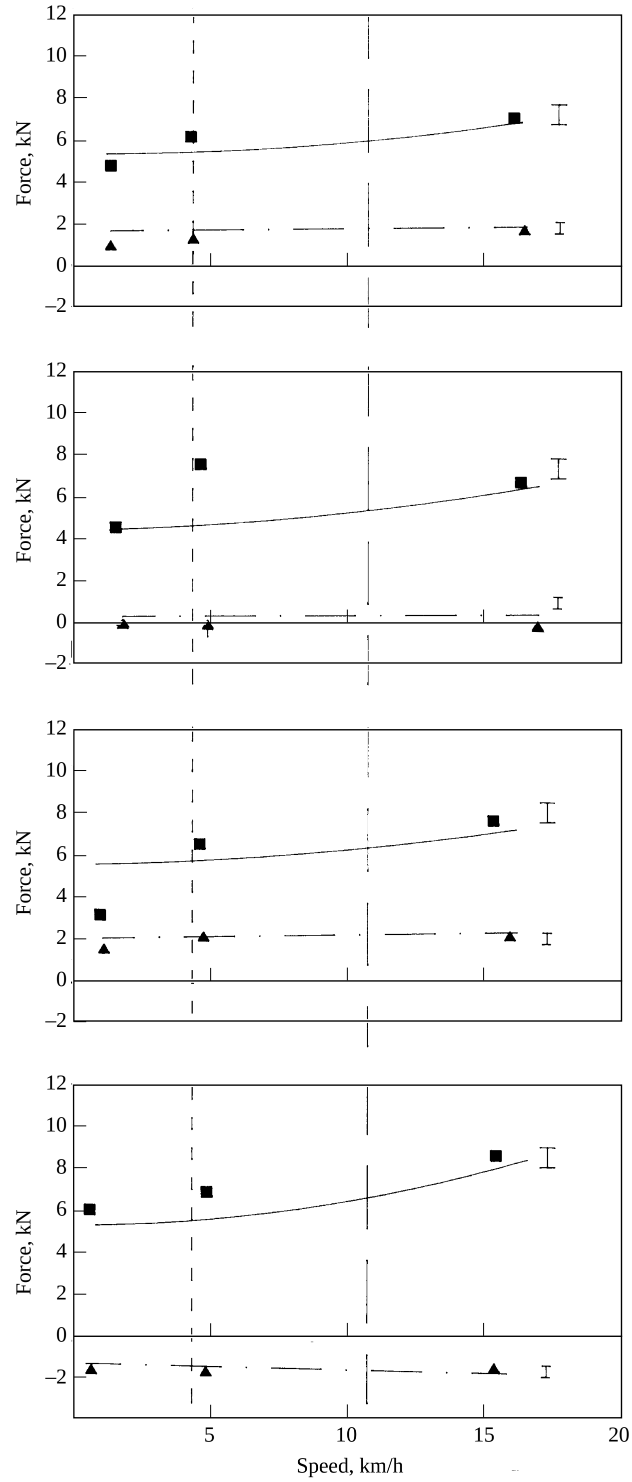

Fig. 8. Effect of speed on forces acting on a single tine with rake angle of 30° (top), 40° (upper centre), 60° (lower centre) and 90° (bottom) in cohesive soil. Also shown are the l.s.d. bands at 0·05 probability level for the experimental data. ■, *Measured horizontal force component;* ▲, *measured vertical force component; ——, predicted horizontal force component; – · –, predicted vertical force component*

(laboratory) soil. Again predicted values show close agreement with the experimental results and in the majority of cases these fall within a band equivalent to the least significant difference of the experimental data at 0·05 probability level.

Table 2
Speeds (km/h) corresponding to 5% and 10% rise in horizontal forces (H_t) and vertical force (V_t)

Tine rake angle α, deg	Frictional soil				Cohesive soil			
	H_t		V_t		H_t		V_t	
	5%	10%	5%	10%	5%	10%	5%	10%
30	6·4	10·00	6·4	10·00	7·2	9·8	5·0	8·6
40	5·6	8·2	6·2	7·1	6·6	9·0	4·5	7·7
60	5·1	6·8	6·0	8·0	6·8	9·3	5·5	9·0
90	4·3	6·5	7·6	8·9	5·0	6·1	7·7	8·9
Mean	5·4	7·9	6·6	8·5	6·4	8·6	5·6	8·6

4. Conclusion

1. The force prediction model developed for single tines working shallower than their critical depth has been shown to give good agreement with the experimental data for both horizontal and vertical components of the resultant force in frictional and cohesive soil conditions at speeds up to 20 km/h.

2. The force model has been shown to give good agreement with the experimental data for the horizontal force acting on multiple tines in frictional soil.

3. The results confirm the findings of Schuring and Emori that inertial forces are insignificant at speeds less than $\sqrt{5gw}$ (4·36 km/h). Modifying this expression to accommodate the effect of soil failure on the sides of narrow tines to $\sqrt{5g(w + 0{\cdot}6d)}$ produces a critical speed of 10·7 km/h for 30 mm wide, 250 mm deep tines.

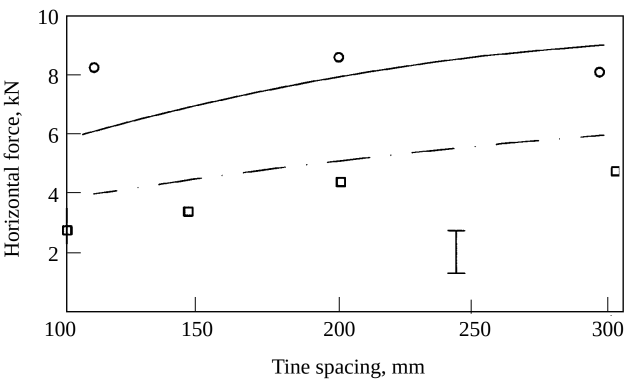

Fig. 9. The effect of tine spacing and speed on horizontal force component acting on multiple tines with a rake angle of 40° in frictional (laboratory) soils at two speeds. Also shown with the l.s.d. band at 0·05 probability level for the experimental data. ○, Measured 20 km/h; □, measured 5 km/h; ——, predicted 20 km/h; – · –, predicted 5 km/h

At this speed the average horizontal force increased by 19% and 14% in frictional and cohesive soils respectively.

Acknowledgements

The assistance given by A. J. Reynolds and the Defence Research Agency is gratefully acknowledged.

References

[1] **Hettiaratchi D R P; Witney B D; Reece A R** The calculation of passive pressure in two-dimensional soil failure. Journal of Agricultural Engineering Research, 1966, **11**(2): 89–107

[2] **Schuring D J; Emori R I** Soil deforming processes and dimensional analysis. 1964. Paper 897c. SAE New York

[3] **Godwin R J; Spoor G** Soil failure with narrow tines. Journal of Agricultural Engineering Research, 1977, **22:** 213–228

[4] **Godwin R J; Spoor G; Soomro M S** The effect of tine arrangement on soil forces and disturbances. Journal of Agricultural Engineering Research, 1984, **30:** 47–56

[5] **McKyes E** Soil Cutting and Tillage. Elsevier, 1985

[6] **Luth H J; Wismer R D** Performance of plane soil cutting blades in sand. Transactions ASAE, 1971, **14**(2): 255–259, 262

[7] **Stafford J V** The performance of a rigid tine in relation to soil properties and speed. Journal of Agricultural Engineering Research, 1979, **24:** 41–56

[8] **Crowther E M; Haines W B** An electrical method for the reduction of draught in plowing. Journal of Agricultural Science, 1924, **14:** 221–231

[9] **King D W** Soils of Bedford and Luton district. Soil Survey of England and Wales, Harpenden, 1969.

[10] **Godwin R J** An extended octagonal ring transducer for use in tillage studies. Journal of Agricultural Engineering Research, 1975, **20**(4): 347–352

[11] **Fisher R A; Yates F** Statistical Tables for Biological, Agricultural and Medical Research. Oliver and Boyd, Edinburgh, 1949